Materials Science and Engineering A 379 (2004) 443–447

www.elsevier.com/locate/msea

Perforation of an ultra-high strength steel penetrated by shaped charge jet

Z.X. Yin [a,b,*], C.M. Ma [c], S.X. Li [b], G.Q. Cheng [b]

[a] *School of Mechanical Engineering, Guangxi University, Nanning 530004, Guangxi Province, PR China*
[b] *Shenyang National Laboratory for Materials Science, Institute of Metal Research, Chinese Academy of Sciences, Shenyang 110016, PR China*
[c] *School of Science, Northeastern University, Shenyang 110006, PR China*

Received 7 August 2003; received in revised form 11 March 2004

Abstract

The "white" etching layer on the perforation surface and adiabatic shear bands (ASBs) in the matrix of ultra-high strength steel plates penetrated by shaped charge jets were investigated. It is shown that the phase transformation took place in the "white" etching layer on the perforation surface during penetration. The microstructure of the "white" etching layer is a mixture of martensite and austenite, both of nanometer scale. The ASBs in the matrix are composed of local shear deformation zones (LSDZs) and heat affect zones (HAZs). No evidence of phase transformation was found in the HAZs of ASBs. The temperature rise on the perforation surface and within ASBs was estimated.

Keywords: Adiabatic shear bands; Shaped charge jets; Ultra-high strength steel

1. Introduction

"White" etching layer or adiabatic shear bands (ASBs) usually develop in metallic materials when loaded by severe impact, such as in machining, impacted plates and projectiles as well as explosively fragmented shells, etc. The formation mechanisms and structural features of ASBs have been of interest to numerous researchers [1–9]. However, considerable controversy exists regarding their structures in steels [3]. In a number of these studies, the bands have been classified as "transformed" or "deformed", depending upon whether they etch white or dark, respectively. Moreover, the shear strain distributions as well as the temperature rises in the ASBs are not well understood. In the present research, the "white" etching layer on the perforation surface and adiabatic shear bands in the matrix of an ultra-high strength steel target plate penetrated by a shaped charge jet are investigated in detail.

2. Experimental

The chemical composition of the steel target material is shown in Table 1. The steel was tempered at 200 °C after quenching to attain a yield stress above 1700 MPa. Its mean hardness is HV 512 and microstructure is martensite with a small amount of carbides. The thickness of the ultra-high strength steel plate is 20 mm. Four such plates were stacked to form a layered target penetrated by a shaped charge jet. The cross-section along the perforation after penetration is shown in Fig. 1. The first and last pieces of the target plates were investigated in detail. Micro-hardness measurement, optical metallography and TEM were employed to analyze the structure changes around the perforation caused by penetration of shaped charge jet.

3. Results and discussion

Fig. 2(a) and (b) shows the structures near the perforations of the first and last target plates, respectively. In Fig. 2(a), the target plate was etched by natal. From the micrograph it is seen that there exists a "white" etching layer on the perforation surface and many adiabatic shear bands emanating from

* Corresponding author. Tel.: +86-77-13272552, +86-13768515813.
E-mail addresses: zhixin5586@sina.com, holly@gxu.edu.cn (Z.X. Yin).

0921-5093/$ – see front matter © 2004 Elsevier B.V. All rights reserved.
doi:10.1016/j.msea.2004.03.032

Table 1
The chemical composition of steel target (wt.%)

	Alloy elements							
	C	Si	Mn	Cr	Mo	S	P	Fe
Content	0.41	0.37	0.28	1.14	0.42	0.002	0.005	Balance

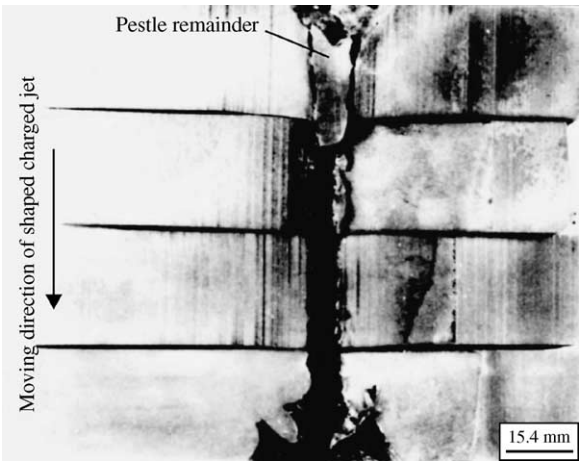

Fig. 1. The cross-section of layered target along the perforation after penetrating by shaped charge jet.

the "white" etching layer into the matrix. Fig. 2(b) shows the last target plate etched by a supersaturated picric acid solution. We can see that the number of adiabatic shear bands in this plate is much smaller than in the first plate. The "white" etching layer on the perforation surface and adiabatic shear bands in the matrix of the steel do not all appear "white" like ones that are etched by natal. However, they both have a clear edge in the matrix of steel. From Fig. 2(b), we can see that there exists a copper layer formed on the outmost layer of the perforation surface. Moreover, there is a central line in the adiabatic shear band. From Fig. 2(b), we also see that whether in the "white" etching layer on the perforation surface or in the adiabatic shear band in the matrix, at their edges the direction of the ghost line of the zonal structure in the matrix of steel target plate almost remains unchanged. However, at the central line of the adiabatic shear band, the direction of the ghost line of the zonal structure changes dramatically. This demonstrates that the shear deformation in ASB is mainly confined to the central line region.

Fig. 3(a) and (b) shows the prior austenite grains of "white" etching layer on the perforation surface and an adiabatic shear band in the matrix of the target, respectively. On the left of Fig. 3(a), the prior austenite grains of the "white" etching layer on the perforation surface are shown, and on the right, the prior austenite grains of the matrix far away from the perforation are seen. From this, besides observing that the majority prior austenite grains are regular and equal axes in shape of mean size about 12 μm, we also find that fine austenite grains of 1–5 μm have been formed at the prior austenite grain boundaries in the "white" etching layer. This demonstrates that re-crystallization of austenite took place in the "white" etching layer on the perforation surface. Obviously, the phase transformation to austenite took place in the "white" etching layer during penetration. Generally speaking, the re-crystallization temperature for austenite in steel is about 950 °C. So, considering the effect of rapid heating on phase transformations in steel, the temperature in "white" etching layer near perforation is estimated to be at least 1000 °C (1273 K).

On the other hand, from Fig. 3(b), we see that the central line of adiabatic shear bands corresponding to the one in Fig. 2(b) actually become a localized shear deformation zone (LSDZ). Its width is about 2 μm. In the light of the displacement of ghost line of zonal structure along central line, it is straightforward to determine the shear strains along the ASB, as shown in Fig. 4. The characteristic of the shear strain, γ, in the LSDZ, from the tip to the tail, gradually increases and then exhibits a reduced rate of increase beyond 1000 μm.

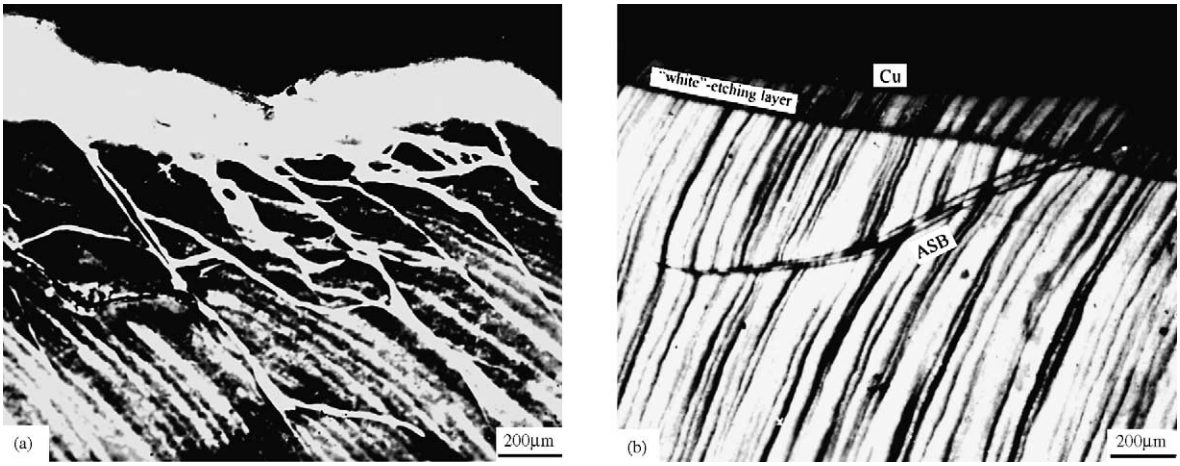

Fig. 2. (a) The structure near the perforation of first target plate etched by natal. (b) The structure near the perforation surface of the last target plate etched by a solution of super-saturated picric acid.

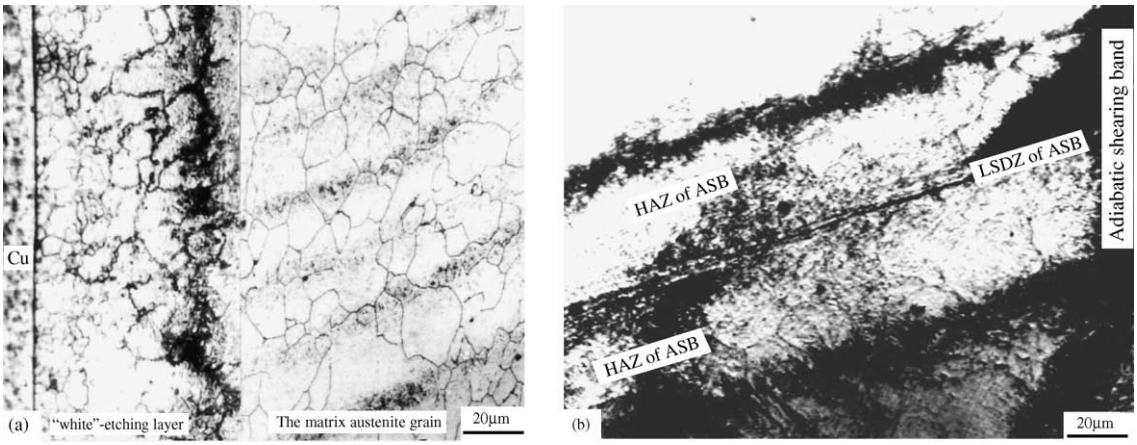

Fig. 3. The characteristic of grains in the austenite in (a) the etching layer and matrix and (b) in the adiabatic shear band.

It is known that the 90% work of shear deformation will be transformed into heat [10] that will result in a temperature increase adjacent to the LSDZ. The temperature rise within the LSDZ caused by adiabatic shear straining can be expressed as follows:

$$\Delta T = k\frac{\tau_{yd}\gamma}{\rho c}$$

where ΔT is the temperature rise, τ_{yd} the dynamic yield shear stress, γ the shear strain, ρ the density and c is the specific heat. Considering that, at the tip of the ASB, there was little effect of the heating, we took the mean shear strain near the tip of ASB as $\gamma = 7$ (from the tip to a distance of 100 μm the shear strain is assumed linear increased from 0 to 14, an average value of 7 is used in the present calculation). The dynamic yielding shear stress can be roughly taken as $\tau_{yd} \approx \sigma_y$ (σ_y is static tensile yielding stress, and equal to 1700 MPa) [11]. From temperature-dependent of the specific heat, we take 1052 J kg^{-1} K^{-1} (at 763 °C) as the specific heat in the calculation. If ρ is 7.8×10^3 kg m^{-3}, and $k = 0.9$, then ΔT is equal to 1350 K. The environment temperature, T_0, is taken as 295 K (22 °C), the temperature what can be reached within LSDZ would be about 1600 K. Although away from the tip the shear strains far exceed seven, due to the lower shear stress caused by thermal softening of the material the temperature may not continue rise with increasing shear strain. So it is considered that it is similar to a constant temperature in the LSDZ while the shear is taking place. That is, it behaves as a heat source with a constant temperature as a function of time along the ASB. It is proposed that the formation of ASBs is an initiation and propagation process [12]. Fig. 5 shows a schematic of ASB formation. We might suppose that an ASB is propagating from right towards left. The shear strain, γ, gradually increases in the LSDZ from the tip to the tail (left to right) and then exhibits a reduced rate of increase, as mentioned above. The maximum temperature, T_{max}, of the heat source in LSDZ is constant, e.g. 1600 K. The duration, t_d, of heating increases with the distance away from the tip of ASB and finally reaches a certain value. With respect to Ref. [1], the duration is estimated as 15 μs, and then heat is no longer added. After that, surrounding material quenches the LSDZ

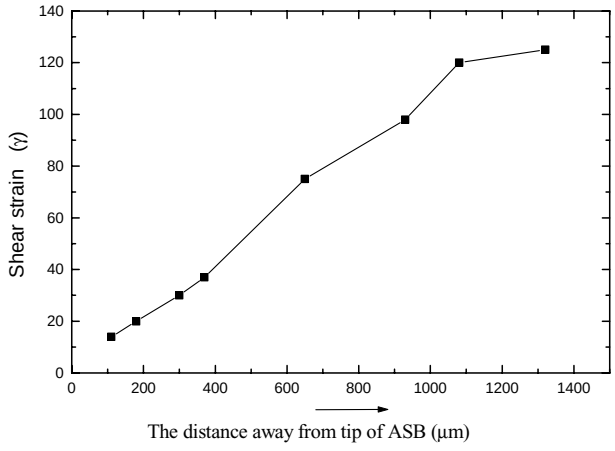

Fig. 4. The variation of shear strains in the LSDZ along its length.

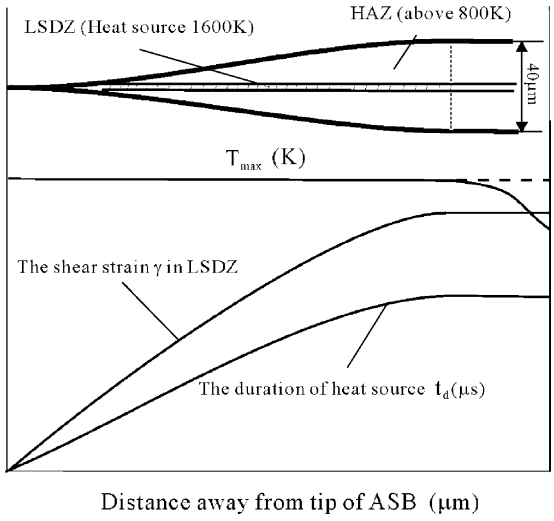

Fig. 5. The schematic diagram of ASB forming.

and the area adjacent to it. Here, we quote the term of fusion welding to name the area as heat affected zones (HAZs). Obviously, T_{max} and the duration of heating, t_d, determine the width of the HAZs. So, it is reasonable that the heat will be conducted away from the center by one-dimensional heat flow in the stable region. The ASB is composed of a localized shear deformation zone (LSDZ) and its heat affected zones (HAZs). The HAZs expands behind the tip, and then grows to some final width with time.

Referring to the heat flow model proposed by Wittman et al. [1], a one-dimensional implicit forward finite-difference program with time steps of 1.4 ns and a node spacing of 0.2 μm was used. The maximum temperature in the LSDZ was 1600 K. From the speed of sound for steel ($3500\,ms^{-1}$) and the whole thickness of the layered target (4 mm × 20 mm), it is estimated that the reflection of the stress waves in the last plate occurred in 29 μs after the impact (the traveling distance of the front wave advancing is $4 \times 20\,mm + 20\,mm$). Thus, the ASB in the last plate would have formed at some time prior to 29 μs after deformation had begun [1]. The temperature–distance profiles at selected times during the heating and cooling processes are shown in Fig. 6. A thermal conductivity, λ, of $44\,W\,m^{-1}\,K^{-1}$ was used. It is shown that, from the LSDZ to the distance of 15–20 μm, the material experienced a temperature higher than 800 K during a period of time (12–50 μs), and this distance is just the half width of the ASB, that is, the half width of HAZs. In the HAZs of an ASB, the white etching of the layer is not a particular indication of a phase transformation; it indicates only that carbides have been dissolved, or are too small to produce localized pitting that would result in dark etching [1].

The maximum temperature at the perforation surface may be estimated according to the width of the white etching layer of the perforation surface. The average width of the "white etching" layer is about 75 μm at the edge of the layer. According to above calculation, it may be suppose that the temperature of the edge of the layer is about 800 K just like at the edge of ASB. Then, if the time spent by heating the surface of the layer is taken as 29 μs (it would be longer than the duration of the heat source in ASB), also referring to the heat flow model proposed by Wittman et al. [1], the highest temperature at the perforation surface would be estimated as 3900 K. That is, the instantaneous temperature at the perforation surface is much high than the melting point of Fe. Recently, it was found that the melting of the perforation surface of carbon steel occurred even in ballistic impact [13]. Therefore, in the present situation, much higher temperature caused by shaped charge jet may be reasonable, even though the estimated value is rather rough.

The micro-hardness of the "white" etching layer, adiabatic shear bands as well as the matrix of the last steel plate is measured. The results are listed in Fig. 7. In order to comparison, the micro-hardness of the untempered martensite of this steel and the ones of the matrixes near the edge of "white" etching layer are also designated in this table. From Fig. 7, it is seen that the values of micro-hardness of both the "white etching" layer and the adiabatic shear bands are lower than those of untempered martensite of the steel. But, they are all higher than the hardness of the matrix. The micro-hardness near the edge of the "white etching" layer is lowest, which perhaps is caused by recovery due to the high temperature affected in the "white etching" layer.

TEM were employed to analyze the microstructure of the "white etching" layer of the perforation surface. The microstructure and corresponding diffraction pattern is shown in Fig. 8. Fig. 8(b) is dark image field of Fig. 8(a). According to analysis of Fig. 8, it can be known that the microstructure of the "white etching" of the perforation surface is mixed, with matensite and retained austenite both present and having nanometer scale (about 20 nm). File data ASTM card and experimentally measured selected-area diffraction data are compared in Table 2. The formation of this microstructure is suggested as follows:

The thermal calculation results indicate that the temperature on the perforation surface is extremely high. Therefore, the cooling rate at the perforation surface is great which

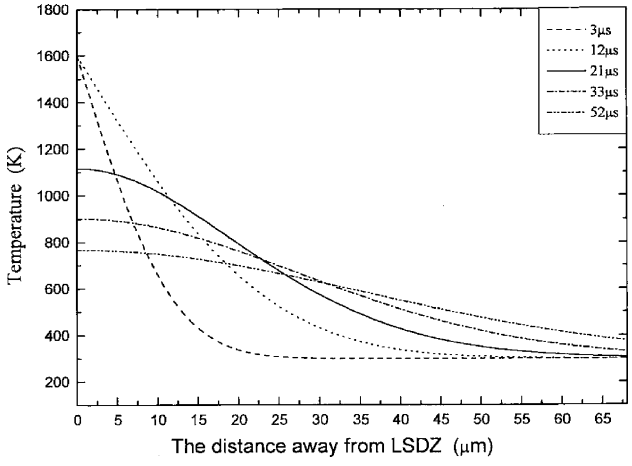

Fig. 6. The temperature profiles at different time near the LSCZ.

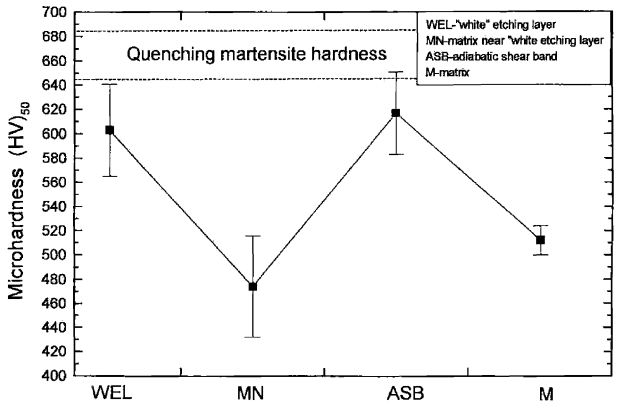

Fig. 7. The distribution of the micro-hardness value of the "white" etching layer on the perforation surface, the matrix near the white etching layer, an adiabatic shear band, as well as the matrix of target.

Table 2
The index of diffraction plane and its interspaces value

Values in ASTM		Values measured		Values in ASTM		Values measured	
d (α-Fe) (nm)	hkl	d (α-Fe) (nm)	hkl	d (γ-Fe) (nm)	hkl	d (γ-Fe) (nm)	hkl
0.20268	110	0.20595	110	0.2080	111	0.20595	111
0.14332	200	0.14604	200	0.1800	200	0.17849	200
0.11702	211	0.12550	211	0.1270	220	0.12550	220
0.10134	220	0.12550	211	0.1080	311	0.10709	311
0.09064	310	0.12550	211	0.1037	222	0.10709	311
0.08275	222	0.08113	222	0.0900	400	0.10709	311

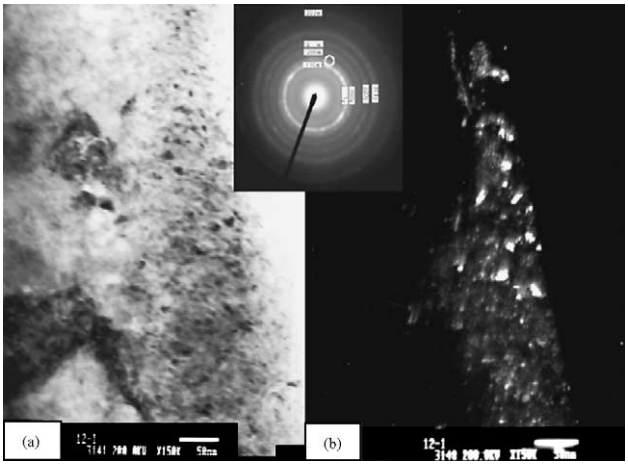

Fig. 8. The TEM structure and diffraction pattern of the "white" etching layer near perforation surface: (a) light image field; (b) dark image field.

leads to the martensite formation. But, these circumstances also result in incomplete martensite formation. For this reason the structure formed is a mixture of martensite and retained austenite, both having nanometer scale.

4. Conclusions

In the present experiments and analysis, some conclusions may be drawn:

1. Due to the extremely high temperature on the perforation surface, the re-crystallization of the austenite within "white" etching layer on the perforation surface of the steel has occurred. The fine austenite grains, 1–5 μm in size, are apparent. Since the cooling rate is very high, a mixture of martensite and retained austenite, both with nanometer scale, is formed. This ultra-fine structure in the "white etching" layer is not as hard as normal, untempered martensite of the steel, due to the presence of retained austenite.
2. The ASB in the matrix of the steel is composed of an LSDZ and a HAZs. The shear strain, γ, in the LSDZ of ASB from the tip to the tail increases gradually and then exhibits a reduced rate of increase. The re-crystallization of austenite in the HAZs was not observed.

Acknowledgements

This research is supported by China Science and Technology Project (95-YJ-14) and China Key Basic Research Project (G19980615). Authors wish to acknowledge the valuable help in TEM observation by Dr. Z.C. Li.

References

[1] C.L. Wittman, M.A. Meyers, H.-R. Pak, Metall. Trans. 21A (1990) 707.
[2] K. Cho, Y.C. Chi, J. Duffy, Metall. Trans. 21A (1990) 1161.
[3] H.C. Rogers, Annu. Rev. Mater. Sci. 9 (1979) 283.
[4] J. Krejci, J. Brezina, J. Buchar, Scripta Metall. Mater. 27 (1992) 611.
[5] G.B. Olson, in: M.A. Meyers, L.E. Mnrr (Eds.), Shock Waves and High-Strain-Rate Phenomena in Metals, Plenum Press, New York, 1981, p. 221.
[6] S.M. Doraivelu, V. Gopinathan, V.C. Venkatesh, in: M.A. Meyers, L.E. Mnrr (Eds.), Shock Waves and High-Strain-Rate Phenomena in Metals, Plenum Press, New York, 1981, p. 263.
[7] K.P. Staudhammer, C.E. Frants, S.S. Hecker, in: M.A. Meyers, L.E. Mnrr (Eds.), Shock Waves and High-Strain-Rate Phenomena in Metals, Plenum Press, New York, 1981, p. 91.
[8] B. Zhang, W. Shen, Y. Liu, Y. Wang, X. Tang, Acta Metall. Sinica 33 (1997) 1161.
[9] J. Shi, H. Dong, Q. Wang, L. Tian, Acta Metall. Sinica 36 (2000) 1045.
[10] C. Fressengeas, A. Molinari, J. Mech. Phys. Solids 35 (1987) 185.
[11] R.J. Clifton, A. Gilat, C.H. Li, in: J. Mescall, N. Weiss (Eds.), Material Behavior under High Stress and Ultrahigh Loading Rates, Plenum Press, New York, 1983, p. 1.
[12] V.F. Nesterenko, M.A. Meyers, T.W. Wright, Acta Mater. 46 (1998) 327.
[13] Z.Q. Duan, S.X. Li, D.W. Huang, Fatigue Fract. Eng. Mater. Struct. 26 (2003) 1119.